



# Dimming Control of LED Light Using Pulse Frequency Modulation in Visible Light Communication

Seong-Ho Lee\* , Member, KIICE

Department of Electronics and IT Media Engineering, Seoul National University of Science and Technology, Seoul 01811, Korea

## Abstract

Light-emitting diodes (LEDs) are modulated using a square wave pulse sequence for flicker prevention and dimming control in visible light communication (VLC). In a VLC transmitter, the high and low bits of the non-return-to-zero (NRZ) data are converted to two square waves of different frequencies, which continue for a finite time defined by the fill ratio in an NRZ bit time. As the average optical power was kept constant and independent of data transmission, the LED was flicker-free. Dimming control is carried out by changing the fill ratio of the square wave in the NRZ bit time. In the experiments, the illumination of the LED light was controlled in the range of approximately 19.2% to 96.2% of the continuous square wave modulated LED light. In the VLC receiver, a high-pass filter combined with a latch circuit was used to recover the transmitted signal while preventing noise interference from adjacent lighting lamps.

**Index Terms:** Dimming control, Fill ratio, Flicker prevention, Light emitting diode, Visible light communication

## I. INTRODUCTION

Visible light communication (VLC) is a new technology in which light sources are used simultaneously for lighting and communication [1-4]. High-power visible light-emitting diodes (LEDs) have been used widely as light sources in various VLC systems. Compared to conventional fluorescent lamps and incandescent lamps, LEDs have high power conversion efficiency, fast response speed, and mechanical safety. VLC systems have several advantages. Specifically, visible light does not interfere with radio frequencies and does not affect other systems outside the illuminated area, and VLC prevents external eavesdropping because the signal is detected within the LED beam. The VLC system should be designed in such a way that lighting and communication do not affect each other because LED lights are used for illumination as well as data transmission [5-7].

The optical power change of an LED light during data

transmission can cause flickering, and the flickering phenomenon should be avoided for comfortable illumination and eye safety. Amplitude-shift keying and frequency-shift keying have been used for flicker prevention [1, 2]. In VLC systems, dimming control is also required to allow the user to change the illumination easily without affecting the communication link. Variable pulse-position modulation and color shift keying approaches have been considered as effective methods for dimming control [1].

In this study, we introduce a simple modulation method that is effective for the flicker prevention and dimming control of LED lights in VLC systems. When the input NRZ data are applied to the transmitter, the high and low bits of the NRZ data are converted to two square waves of different frequencies, and the square waves continue for a finite time, which is defined by the fill ratio in an NRZ bit time. The proposed scheme is called pulse-frequency modulation (PFM).

In PFM, the average optical power of the LED light is


Received 23 September 2021, Revised 06 November 2021, Accepted 06 November 2021

\*Corresponding Author Seong-Ho Lee (E-mail: [shlee@seoultech.ac.kr](mailto:shlee@seoultech.ac.kr), Tel: +82-2-970-6457)

Department of Electronics and IT Media Engineering, Seoul National University of Science and Technology, Seoul 01811, Korea.

**Open Access** <https://doi.org/10.6109/jicce.2021.19.4.269>

print ISSN: 2234-8255 online ISSN: 2234-8883

 This is an Open Access article distributed under the terms of the Creative Commons Attribution Non-Commercial License (<http://creativecommons.org/licenses/by-nc/3.0/>) which permits unrestricted non-commercial use, distribution, and reproduction in any medium, provided the original work is properly cited.

Copyright © The Korea Institute of Information and Communication Engineering

independent of the number of high and low bits in the NRZ data, and it remains constant regardless of whether the data is transmitted, and the illumination maintains a flicker-free state. When it is necessary to change the LED illumination, a different fill ratio is selected by changing the duration of the square wave in the bit time. This configuration is useful in constructing indoor VLC systems using LED lamps, particularly in exhibition halls or department stores, where the product information is transmitted wirelessly to guest smartphones via the LED light within a booth without affecting the neighboring store.

## II. PULSE FREQUENCY MODULATION

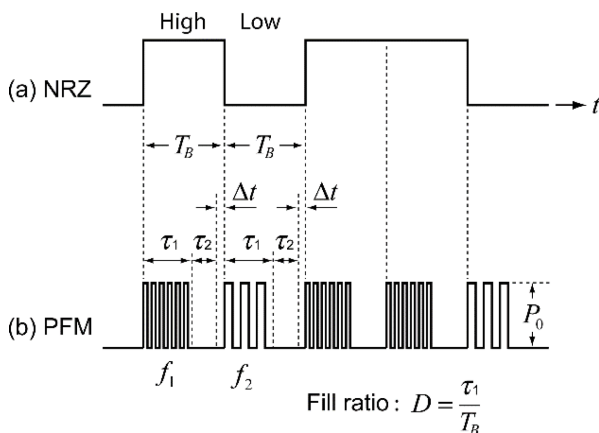
In the VLC transmitter using PFM transmission, NRZ input data bits are converted to square waves of two different frequencies, and the square wave continues for a finite time, which is defined by the fill ratio. Fig. 1 shows the conversion from the NRZ data to the PFM signal.

Fig. 1(a) is an arbitrary NRZ waveform with a bit time of  $T_B$ . Fig. 1(b) shows the PFM waveform in which the high and low NRZ bits are converted to square waves with repetition frequencies  $f_1$  and  $f_2$ , respectively.  $\tau_1$  represents the on-time for which the PFM waveform continues;  $\tau_2$  denotes the off-time in which the PFM signal does not exist, and  $\Delta t$  indicates the interval between adjacent bits. In these waveforms, the one-bit time of the NRZ waveform can be expressed as follows:

$$T_B = \tau_1 + \tau_2 + \Delta t. \tag{1}$$

In the PFM waveform in Fig. 1(b), the fill ratio can be defined as:

$$D = \frac{\tau_1}{T_B}. \tag{2}$$



**Fig. 1.** Illustration of pulse-frequency modulation. (a) Non-return-to zero input waveform and (b) optical power of a light emitting diode in pulse-frequency modulation.

If  $m$  high bits and  $n$  low bits in the NRZ waveform are transmitted during an observation time of  $T$ , the average optical power of the LED light in the PFM waveform can be obtained as follows:

$$\begin{aligned} P_{avg} &= \frac{1}{T} \int_0^T P(t) dt \\ &= \frac{1}{T} \left( m \int_0^{T_B} P_H(t) dt + n \int_0^{T_B} P_L(t) dt \right) \\ &= \frac{1}{T} \left( m \int_0^{\tau_1} P_H(t) dt + n \int_0^{\tau_1} P_L(t) dt \right) \\ &= \frac{P_0}{T} \left( \frac{m\tau_1}{2} + \frac{n\tau_1}{2} \right). \end{aligned} \tag{3}$$

where  $P_{avg}$  represents the average optical power;  $P(t)$  denotes the instantaneous optical power of the LED light, and  $P_H(t)$  and  $P_L(t)$  are square wave functions with frequencies  $f_1$  and  $f_2$ , respectively.  $P_0$  corresponds to the optical amplitude of the LED light modulated by the PFM waveform;  $\tau_1$  is the on-time of the PFM waveform, and  $m$  and  $n$  are the numbers of the NRZ high and low bits in the observation time  $T$ . The observation time  $T$  is equal to  $(m + n) T_B$ , where  $T_B$  is one NRZ bit time, and Equation (3) becomes:

$$\begin{aligned} P_{avg} &= \frac{P_0}{(m+n)T_B} \left( \frac{m\tau_1}{2} + \frac{n\tau_1}{2} \right) = \frac{P_0}{(m+n)T_B} (m+n) \frac{\tau_1}{2} \\ &= \frac{P_0}{2} \times \frac{\tau_1}{T_B} = \frac{P_0}{2} \times D = P_m \times D. \end{aligned} \tag{4}$$

where  $P_m$  is the maximum average optical power when the LED light is modulated by a square wave. Specifically, it is,  $P_m = P_0/2$ , and  $D$  corresponds to the fill ratio of the PFM waveform defined in equation (2). As shown in equation (4), the average optical power of the LED light is independent of the bit numbers  $m$  and  $n$ ; therefore, it is independent of the NRZ bit state and remains constant. As a result, the LED light remains flicker-free while the fill ratio is fixed at a specific value. During the experiment, the average optical power changed linearly with the fill ratio, and the illumination was controlled by changing the fill ratio. The relationship between the average optical power and the fill ratio is shown in Fig. 2.

In Fig. 2, the solid line was calculated using equation (4), and the symbol (■) represent the measured data in the experiments. For the measurements, we used a square wave with a frequency  $f_1 = 100$  kHz for the NRZ high bit, in which the pulse width was  $5 \mu s$  and the pulse period was  $10 \mu s$ . For the NRZ low bit, a square wave with frequency  $f_2 = 50$  kHz was used, in which the pulse width was  $10 \mu s$  and the pulse period was  $20 \mu s$ . The NRZ data rate was 9.6 kbps, where the one-bit time ( $T_B$ ) was  $104 \mu s$ . The interval time between adjacent bits ( $\Delta t$ ) was  $4 \mu s$ .

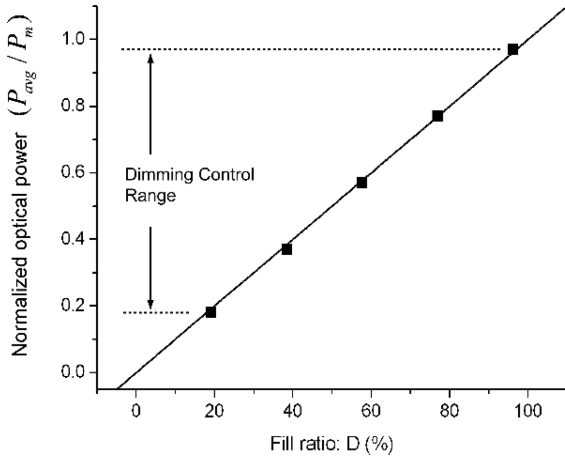


Fig. 2. Average optical power change with fill ratio.

We increased the on-time  $\tau_1$  of the PFM waveform by 20  $\mu$ s stepwise from 20  $\mu$ s to 100  $\mu$ s to measure the average optical power change with the fill ratio. Under these conditions, the lowest fill factor was  $D_{min} = \tau_{1,(min)}/T_B = 20/104 = 19.2\%$ , and the highest fill factor was  $D_{max} = \tau_{1,(max)}/T_B = 100/104 = 96.2\%$ . As shown in Fig. 2, the average optical power of the LED light exhibited an approximately linear relationship with the fill ratio. In the measurements, the optical power density was measured as the fill ratio was changed, and the measured data were normalized to the maximum value of the square wave light  $P_m = P_0/2$ , where  $P_0$  is the optical amplitude of the LED. The maximum power density  $P_m$  was measured to be approximately 0.4 W/m<sup>2</sup> at a distance of approximately 2 m from the LED array, and the illumination was approximately 300 lx. The optical power density and illumination were measured using an optical multimeter (OMM-6810B) and an illuminance meter (UT382).

### III. SYSTEM CONFIGURATION

#### A. VLC Transmitter

Fig. 3 is the illustration of the VLC transmitter configuration.

The VLC transmitter comprised a PFM modulator, a current driver, and an LED array. A microcontroller, Atme-

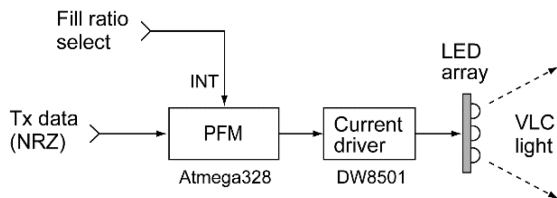


Fig. 3. Configuration of the transmitter.

ga328, was used as the PFM modulator and a DW8501 integrated circuit was used for the current driver. The LED array was in a 3×4 planar array form, which was composed of twelve 1 W white LEDs. When the NRZ data was applied to the input of the transmitter, the PFM modulator converted each bit of the NRZ data into square waves of frequencies 10 kHz and 5 kHz, and these were used for the high and low NRZ bits, respectively.

The PFM signal continued for a finite time ( $\tau_1$ ), which was defined by the fill ratio within an NRZ bit time. The fill ratio was selected by transmitting interrupt pulses to Atmega328, in which the on-time  $\tau_1$  of the PFM waveform increased by 20  $\mu$ s stepwise for each interrupt pulse from  $\tau_1 = 20 \mu$ s to  $\tau_1 = 100 \mu$ s in an NRZ bit time of  $T_B = 104 \mu$ s. The NRZ bit time corresponds to a 9.6 kbps data rate. The PFM signal was applied to the input of the current driver, and the output current was supplied to the LED array, whose output light radiates to the VLC receiver through free space. We repeatedly sent the character “K” to confirm the operation of the transmitter and observed the voltage waveforms using an oscilloscope, as shown in Fig. 4.

Fig. 4(a) shows the NRZ data waveform for the character “K”. The ASCII code for the character “K” is 01001011. In UART transmission, the least significant bit is transmitted first, and the bit sequence is reversed to 11010010. A start bit (0) was added in front of the character and a stop bit (1) was added at the end; thus, a ten-bit NRZ bit sequence 0110100101 was transmitted for character “K”. When high (H) and a low (L) voltages were assigned to “1” and “0” bits, respectively, the voltage signal became LHHLLHLLH, as shown in Fig. 4(a).

Fig. 4(b) to (d) illustrate the PFM waveforms. An NRZ high bit was converted to a square wave of frequency  $f_1 = 100$  kHz, in which the rectangular pulses with a pulse-width of 5  $\mu$ s are repeated with a period of 10  $\mu$ s during the on-time  $\tau_1$ . An NRZ low bit was converted to a square wave of frequency  $f_2 = 50$  kHz, in which the rectangular pulses with a pulse-width of 10  $\mu$ s repeated with a period of 20  $\mu$ s during the on-time  $\tau_1$ . The NRZ bit time ( $T_B$ ) was 104  $\mu$ s, and the interval time between adjacent bits ( $\Delta t$ ) was set to 4  $\mu$ s.

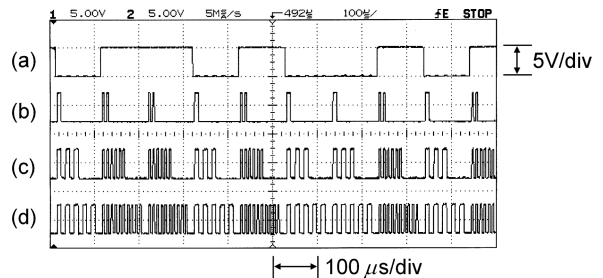


Fig. 4. Waveforms observed in the transmitter. (a) Non-return-to zero data waveform and pulse-frequency modulation waveforms with fill ratio of (b)  $D = 19.2\%$ , (c)  $D = 57.6\%$ , and (d)  $D = 96.2\%$ .

In Fig. 4(b), the on-time of the PFM waveform is  $\tau_1 = 20 \mu\text{s}$  and the fill ratio is  $D = \tau_1/T_B = 20/104 = 19.2\%$ ; thus, two pulses appear in the NRZ high bit and one pulse appears in the NRZ low bit. In Fig. 4(c), the on-time of the PFM waveform is  $\tau_1 = 60 \mu\text{s}$ , the fill ratio is  $D = \tau_1/T_B = 60/104 = 57.6\%$ . Accordingly, six pulses appear in the NRZ high bit and three pulses appear in the NRZ low bit. In Fig. 4(d), the on-time of the PFM waveform is  $\tau_1 = 100 \mu\text{s}$  and the fill ratio is  $D = \tau_1/T_B = 100/104 = 96.2\%$ ; thus, ten pulses appear in the NRZ high bit and five pulses appear in the NRZ low bit.

**B. VLC Receiver**

A VLC receiver that was installed at a distance of approximately 2 m from the LED array was used to detect the light emitted from the LED, which was modulated by the PFM signal. Fig. 5 shows the circuit diagram of the VLC receiver.

The VLC receiver comprised a photodiode (PD), three amplifiers, an RC high-pass filter (RC-HPF), two diodes, an SR-latch circuit, and a microcontroller. In the experiments, we used an S6968 PIN PD, three OPA228 op-amps, two 1N4148 diodes, an Atmega328 microcontroller, and an SR-latch circuit consisting of two NAND gates.

When the VLC light from the transmitter arrived at the receiver, an amplified PD voltage passed through the RC-HPF to cut off the 120 Hz noise passed through the RC-HPF. Owing to the differential operation of the RC-HPF, positive and negative spikes appeared at the rising and falling edges of the rectangular pulses of the PFM waveform, respectively. The spike voltage at the output of the RC-HPF was simultaneously applied to the input ports of amp-1 and

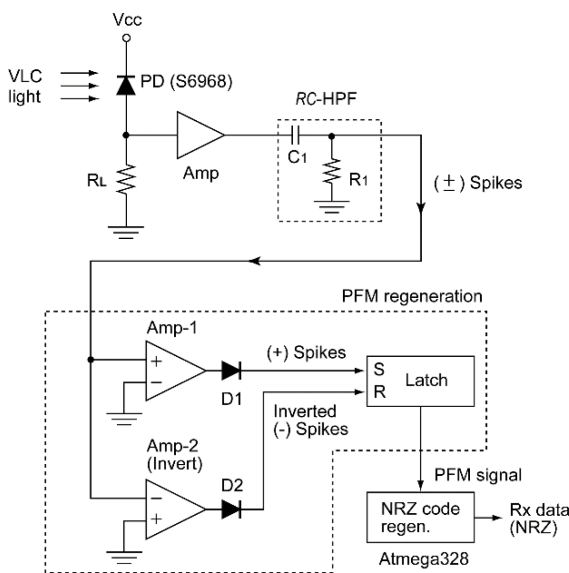


**Fig. 5.** Configuration of the receiver.

amp-2. Moreover, amp-1 and amp-2 are non-inverting and inverting amplifiers, respectively.

The output of the non-inverting amplifier (amp-1) passed through diode  $D_1$ ; the positive spike passed through it while the negative spike was cut off. Thus, only the positive spike from the RC-HPF was applied to the  $S$  input of the SR-latch circuit. Similarly, the output voltage of the inverting amplifier (amp-2) passed through diode  $D_2$ ; the inverted negative spike passed through it while the inverted positive spike was cut off. As a result, only the inverted negative spike from the RC-HPF was applied to the  $R$  input of the SR latch circuit.

A positive spike transits the SR-latch output to a high voltage state while a negative spike transits it to a low voltage state. As a result, the PFM signal sent from the transmitter was regenerated at the output of the SR-latch while the 120 Hz noise was cut off by the RC-HPF. We observed the voltage waveforms in the VLC receiver to confirm the regeneration of the PFM signal. Fig. 6 illustrates the voltage waveforms observed using an oscilloscope.

Fig. 6(a) shows the PD voltage when the LED light was modulated by the PFM waveform with a fill ratio of 57.6% in the transmitter. Fig. 6(b) shows the output voltage of the HPF, Fig. 6(c) shows the positive spikes appearing at the output of diode  $D_1$ ; Fig. 6(d) depicts the inverted negative spikes at the output of diode  $D_2$ , and Fig. 6(e) shows the PFM waveform regenerated by the SR-latch circuit.

The regenerated PFM signal was applied to the interrupt port of the microcontroller. Afterward, the NRZ data was recovered. The recovery process of the NRZ data from the PFM signal is schematically illustrated in Fig. 7.

As shown in Fig. 7(a), at each rising edge of the rectangular pulses in the PFM signal, the microcontroller reads the voltage level two times sequentially from the rising edge with an interval of  $5 \mu\text{s}$ , which is the same as the pulse width of the PFM signal for the NRZ high bit. If the two readings are equal to (1, 0), the microcontroller transitions to a high voltage state and continues until a new data (1, 1) reading is made. When the read data is equal to (1, 1), the microcontroller transitions to a low voltage state and continues until a new data (1, 0) reading is made. In this manner, the microcontroller recovered the NRZ data waveform from

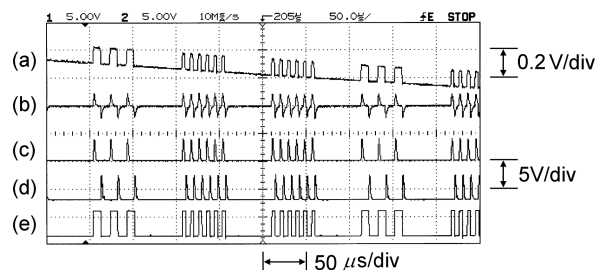


**Fig. 6.** Waveforms observed in the receiver with a fill ratio of  $D = 57.6\%$ . (a) Photodiode voltage, (b) high-pass filter output, (c) positive spikes, (d) inverted negative spikes, and (e) regenerated pulse-frequency modulation waveform.

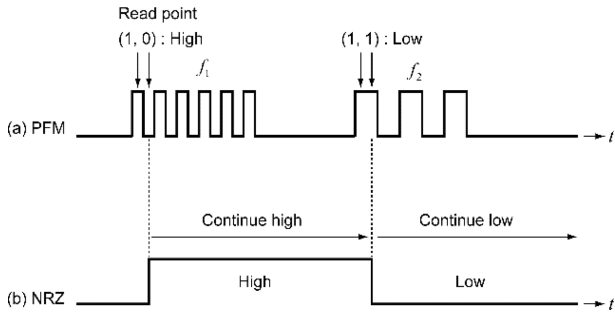


**Fig. 7.** Recovery process of the non-return-to-zero waveform from the pulse-frequency modulation signal.

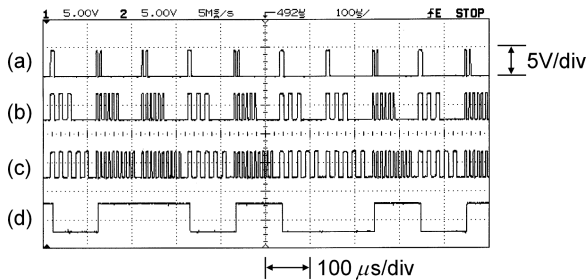


**Fig. 8.** Waveforms observed in the receiver. Pulse-frequency modulation waveforms with fill ratio of (a)  $D = 19.2\%$ , (b)  $D = 57.6\%$ , and (c)  $D = 96.2\%$ . (d) Non-return-to-zero waveform recovered by the microcontroller.

the PFM signal, as illustrated in Fig. 7(b).

We observed the regenerated PFM and NRZ data waveforms as the fill ratio of the PFM waveform changed in the transmitter. Fig. 8 illustrates the PFM signal and regenerated NRZ waveforms observed using an oscilloscope.

Fig. 8(a), (b), and (c) correspond to the PFM waveforms recovered by the SR-latch circuit in the VLC receiver when the fill ratio was  $D = 19.2\%$ ,  $57.6\%$ , and  $96.2\%$ , respectively. Fig. 8(d) shows the recovered NRZ waveform for the character “K”. The recovered NRZ waveform is the same while the fill ratio changes, and it is equal to the NRZ waveform transmitted by the transmitter, as shown in Fig. 4(a). Thus far, we experimentally confirmed the PFM wave generation process in the transmitter, the recovering process of the PFM waveforms, and the conversion from PFM to NRZ data bits in the receiver.

#### IV. TRANSMISSION EXPERIMENTS

The PFM method was applied to data transmission from an LED array to a smartphone. The configuration can be used for indoor wireless data transmission to provide product information to guests in an exhibition hall or department store using an LED lamplight. Each booth had a lighting lamp. As the data can be received within the area where the LED light reaches, the data was transmitted within the booth

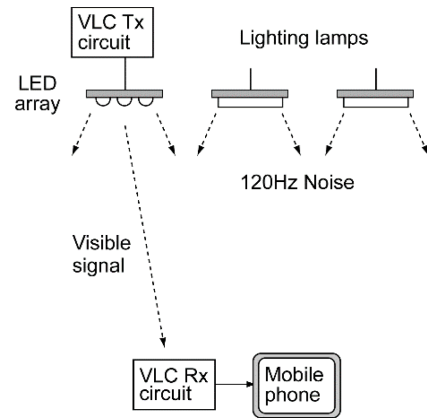


**Fig. 9.** Experimental setup.

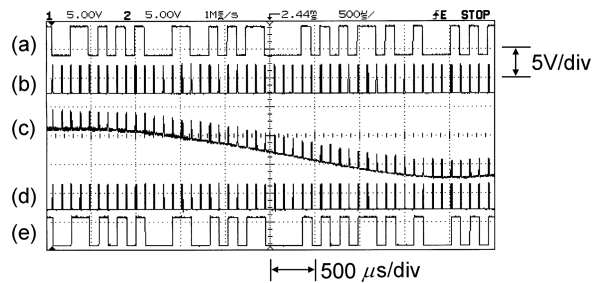


**Fig. 10.** Waveforms observed in the transmitter and receiver. (a) Non-return-to-zero signal and (b) pulse-frequency modulation signal in the transmitter. (c) Photo-diode voltage, (d) regenerated pulse-frequency modulation signal, and (e) recovered non-return-to-zero signal in the receiver.

without interfering with the neighbor. The experimental setup is illustrated in Fig. 9.

The LED array in the VLC transmitter was installed near the ceiling, beside other lighting lamps in the laboratory. The signal light of the LED array was modulated by the PFM signal of the transmitted data. Other lighting lamps that were not concerned with data transmission were also installed on the ceiling near the VLC transmitter, and the light from these lighting lamps contained 120 Hz noise.

The VLC receiver was installed on a table at a distance of approximately 2 m from the VLC transmitter. The light from the VLC transmitter and those from other lighting lamps were mixed at the position of the VLC receiver. A character string “VLC-TX-test\r\n” was transmitted repeatedly at a 9.6 kbps data rate, and the voltage waveforms in the transmitter and the receiver were observed using an oscilloscope, as shown in Fig. 10.

Fig. 10(a) shows the NRZ waveform in the transmitter. Fig. 10(b) depicts the PFM waveform with a fill ratio of 19.2% in the transmitter. Fig. 10(c) shows the photodiode voltage, in which the PFM waveform is mixed with the 120 Hz noise from adjacent lighting lamps. This signal cannot be directly received owing to noise interference, and an RC-HPF was used to cut off the 120 Hz noise. Fig. 10(d) shows

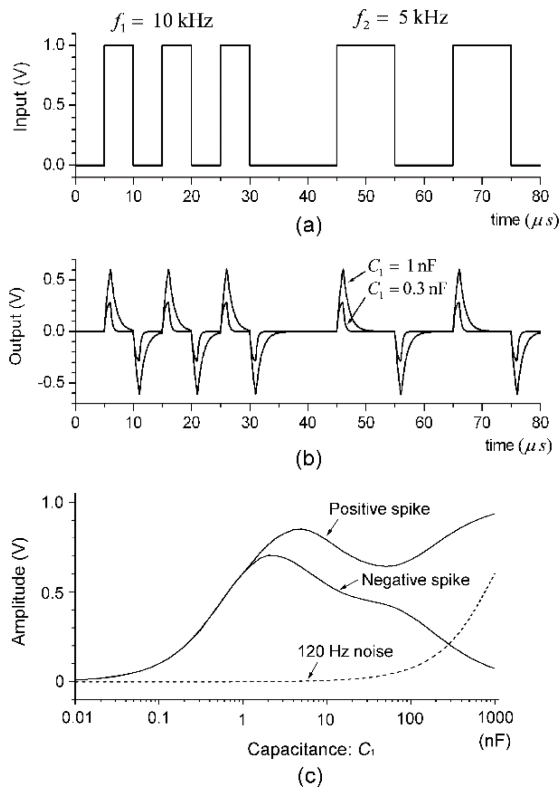


**Fig. 11.** Simulation results of a high pass filter. (a) Input voltage, (b) output spike voltage, and (c) peak amplitude change with capacitance.

the regenerated PFM waveform without the noise using an RC-HPF and an SR-latch circuit in the VLC receiver. Fig. 10(e) shows the regenerated NRZ data waveform in the receiver.

We simulated the filter waveforms using the PSpice program to find the optimum capacitance in the RC-HPF. Fig. 11 shows the simulation results.

Fig. 11(a) shows the square wave input voltage in the PFM signal with frequencies of 10 kHz and 5 kHz. Fig. 11(b) illustrates the spike voltages at RC-HPF output with the capacitances  $C_1 = 1 \text{ nF}$  and  $0.3 \text{ nF}$  when the resistance was fixed at  $R_1 = 1 \text{ k}\Omega$ . Fig. 11(c) depicts the amplitude changes of spikes and 120 Hz noise with capacitance  $C_1$ . The positive and negative spike amplitudes are almost equal and maximum while the 120 Hz noise disappeared when the capacitance was approximately 1 to 2 nF. Thus, we used  $C_1 = 1 \text{ nF}$  and  $R = 1 \text{ k}\Omega$  in RC-HPF.

The recovered NRZ waveform in Fig. 10(e) was applied to the USB input port of a smartphone through a serial-to-USB converter. Fig. 12 shows the LED array used as the light source in VLC transmitter and the receiver circuit including a photodiode and a smartphone.

Fig. 12(a) shows the LED array installed near the ceiling of the laboratory, and it was used as a light source in the VLC transmitter. Fig. 12(b) illustrates the VLC receiver cir-

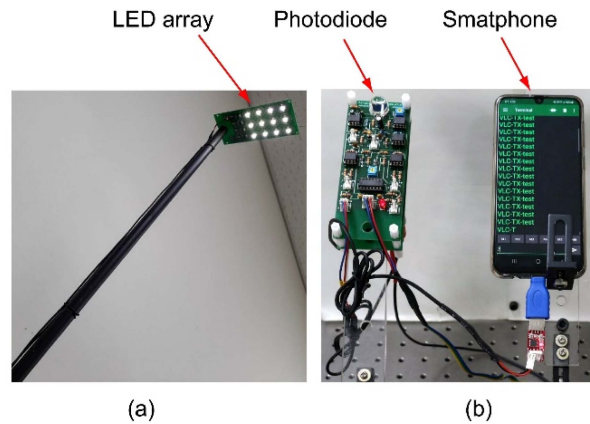


**Fig. 12.** Devices used in experiments. (a) Light emitting diode array in transmitter and (b) receiver circuits, including a photodiode and smartphone.

cuit, including a photodiode and a smartphone. Moreover, the characters sent by the transmitter are displayed on the screen of a smartphone. The two characters “\r” and “\n” in the transmitted data are special characters for position control and are not shown. The remnant characters “VLC-TX-test” are displayed on the screen of a smartphone, as shown in Fig. 12(b).

## V. DISCUSSION AND CONCLUSIONS

In this study, we developed a new PFM transmission method for the flicker-prevention and dimming control of an LED light source in visible light communication. The high and low bits in the NRZ data are converted to square waves of two different frequencies, and the duration of the square wave in a bit time is selected by the user to control the illumination of the LED light. It was confirmed that when the fill ratio is fixed at a specific value, the average optical power of the LED light remained constant and flicker-free. When the user wants to change the illumination of the LED, a different fill ratio is selected by pressing a push-button switch to apply interrupt signals to the transmitter. In the experiments, the illumination was controlled in the range of 19.2% to 96.2% of the square wave modulated LED light.

An RC-HPF was used in the VLC receiver to eliminate the interference of the 120 Hz noise from the adjacent light lamps. The RC-HPF cuts off the noise interference; however, the differential operation in the RC-HPF distorts the square wave in the PFM signal. If signal distortion is severe, the output of the RC-HPF cannot be directly used for data recovery. In this state, the spike voltages at the HPF output were utilized to recover the square waves in the PFM signal. In the experiments, when the 120 Hz noise amplitude was approximately twice that of the PFM signal, the square wave was effectively recovered while cutting off the noise using an RC-HPF and an SR-latch circuit.

The configuration introduced in this study can be used widely in constructing indoor wireless communication links in an exhibition hall or department store to provide product information to guest smartphones using LED lamps as the VLC transmitter. It was confirmed that the VLC system in each booth operates safely without interfering with the neighbor because the VLC signal is detected only within the LED light beam and does not pass through the booth wall.

## ACKNOWLEDGMENTS

This study was supported by the Research Program funded by the SeoulTech (Seoul National University of Science and Technology).

## REFERENCES

- [ 1 ] S. Rajagopal, R. D. Roberts, and S. K. Lim, "IEEE 802.15.7 visible light communication: modulation schemes and dimming support," *IEEE Communications Magazine*, vol. 50, no. 3, pp. 72-82, 2012. DOI: 10.1109/MCOM.2012.6163585
- [ 2 ] C. Yao, Z. Guo, G. Long, and H. Zhang, "Performance comparison among ASK, FSK and DPSK in visible light communication", *Optics and Photonics Journal*, vol. 6, no. 8B, pp. 150-154, 2016. DOI: 10.4236/opj.2016.68B025.
- [ 3 ] S. Li, A. Pandharipande, and F. M. J. Willems, "Unidirectional visible light communication and illumination with LEDs", *IEEE Sensors Journal*, vol. 16, no. 23, pp. 8617-8626, 2016. DOI: 10.1109/JSEN.2016.2614968.
- [ 4 ] A. M. Cailean and M. Dimian, "Current challenges for visible light communications usage in vehicle applications: A survey", *IEEE Communications Surveys & Tutorials*, vol. 19, no. 4, pp. 2681-2703, 2017. DOI: 10.1109/COMST.2017.2706940.
- [ 5 ] S. H. Lee, "A passive transponder for visible light identification using a solar cell", *IEEE Sensors Journal*, vol. 15, no. 10, pp. 5398-5403, 2015. DOI: 10.1109/JSEN.2015.2440754.
- [ 6 ] Y. K. Cheong, X. W. Ng, and W. Y. Chung, "Hazardless biomedical sensing data transmission using VLC", *IEEE Sensors Journal*, vol. 13, no. 9, pp. 3347-3348, 2013. DOI: 10.1109/JSEN.2013.2274329.
- [ 7 ] V. P. Rachim, Y. Jiang, H. S. Lee, and W. Y. Chung, "Demonstration of long-distance hazard-free wearable EEG monitoring system using mobile phone visible light communication", *Optics Express*, vol. 25, no. 2, pp. 713-719, 2017. DOI: 10.1364/oe.25.000713.



### Seong-Ho Lee

is a professor at the Department of Electronics and IT Media Engineering, Seoul National University of Science and Technology, Korea. He received his BS degree from Korea Aerospace University in 1980, and received his MS and PhD degrees from KAIST, Korea, in 1989 and 1993, respectively. His current research interests include noise reduction, flicker prevention, and dimming control in visible light communication and visible light identification systems.